ISBN: 978-3-95450-230-1 ISSN: 2673-5350 doi:10.18429/JACoW-IBIC2021-WEPP23

DESIGN OF WALL CURRENT MONITOR IN BRing AT HIAF

Peilin He†, Yongliang Yang, Xincai Kang, Xiaotao Liu, Zhiguo Xu, Ruishi Mao
Institute of Modern Physics, Chinese Academy of Sciences, Lanzhou, China

Abstract

The Wall Current Monitor (WCM) can monitor the longitudinal beam shape, beam stability, beam longitudinal emittance and intensity, which has been applied widely in the laboratories of high-current proton accelerators. Many accelerators such as CERN-PS, CERN-CLIC, J-PARC and CSNS-RCS have designed different WCMs according to their respective accelerator beam parameters. In order to provide the high-intensity heavy-ion accelerator facility (HIAF)-BRing high-frequency system of with the intensity of each harmonic beam to compensate for wake field; and to observe the changes of the bundle length during the injection, acceleration, and extraction of the bundle, it is planned to place a WCM in HIAF-BRing. According to physical requirements, the lower limit of the WCM working bandwidth is expected to reach 10 kHz, and the upper limit can reach 100 MHz. According to this bandwidth requirement, a WCM structure is designed, and its theoretical bandwidth is 2 kHz~400 MHz, which fully meets the demand. This article gives a detailed and comprehensive introduction to the overall design of this WCM, the selection of various components, design calculations and related simulation calculations. At present, the WCM has completed the procurement and processing of various components, while offline and online testing has not been carried out owing to time constraints. It is expected to be installed on the Heavy Ion Research Facility in Lanzhou-Cooling Storage Ring (HIRFL-CSR) for online testing in August.

PRINCIPLE OF WCM

When the beam passes through the vacuum pipe, its AC component will produce a constant-amplitude and inverse-phase mirror current on the wall of the vacuum pipe. The WCM uses this principle to measure the longitudinal information of the beam. Its schematic diagram and the corresponding equivalent circuit are shown in Fig. 1.

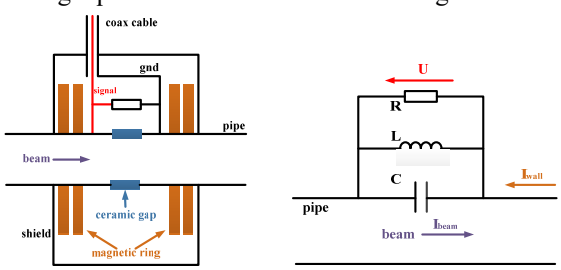

Figure 1: the schematic diagram and the corresponding equivalent circuit of WCM.

Cut the vacuum pipe and install a section of ceramic ring, connecting a resistor across the two ends of the ceramic ring, the induced wall current(mirror current) will produce a voltage which is proportional to the beam current on this resistor. By directly measuring the voltage signal, the intensity signal of the beam pulse can be measured [1].

Ceramic Gap

The main purpose of adding a ceramic ring is to isolate the vacuum pipe, making the induced wall current flow to the resistance. In addition, after welding with the vacuum pipe, it can also make the magnetic ring, shield and other parts outside the vacuum, which makes it easy to control the vacuum performance index of the whole device.

Its equivalent capacitance value is:

$$C_{gap} = (\varepsilon_0 \varepsilon_r S)/t \tag{1}$$

The characteristic impedance of the ceramic ring is:

$$Z = 377 \frac{t}{2\pi r_0} \frac{1}{\sqrt{\varepsilon_r}} \tag{2}$$

Where ε_0 is the vacuum dielectric constant, ε_r is the relative dielectric constant, S and t are the side area and thickness of the ceramic ring. $r_0 = (r_{in} + r_{out})/2$, r_{in} and r_{out} are the inner and outer radius of the ceramic ring.

Magnetic Ring

The magnetic ring is filled outside the vacuum pipe and inside the shielding shell, acting as a role to increase the inductance. Its equivalent inductance value is:

$$L = \frac{\mu_0 \mu_r}{2\pi} h \ln(\frac{b}{a}) \tag{3}$$

Where μ_0 is the vacuum permeability, μ_r is the relative permeability，h is the thickness of the magnetic ring，a and b are the inner and outer diameter of the magnetic ring.

Signal Pick-up Resistance

Because resistors have certain inductance and capacitance characteristics under high frequency, the signal pickup resistor of WCM uses multiple non-inductive resistors connected across the ceramic gap in parallel, and in order to achieve matching, the equivalent resistance value R must be equal to the characteristic impedance Z of the ceramic ring.

Working Bandwidth

Upper cutoff frequency:

$$f_H = \frac{1}{2\pi R C_{gap}} = \frac{r_0}{377 S \varepsilon_0 \sqrt{\varepsilon_r}} \tag{4}$$

Lower cutoff frequency:

† hpl@impcas.ac.cn

ISBN: 978-3-95450-230-1 ISSN: 2673-5350 doi:10.18429/JACoW-IBIC2021-WEPP23

$$f_L = \frac{R}{2\pi L} = \frac{R}{\mu_0 \mu_r h \ln(\frac{b}{a})} \quad (5)$$

DESIGN OF WCM

Ceramic Ring Size Calculation

The ceramic ring material is 97 ceramic, ε_r=9.5 , din (inner diameter) is equal to the diameter of the vacuum pipe, 200 mm. The various indicators of the ceramic ring are analyzed as shown in Fig. 2. Figure 2(a) shows that when t is constant, the influence of dout/din on f_H and Z; Fig. 2(b) shows that when the inner and outer diameters are constant , the influence of t on f_H and Z.

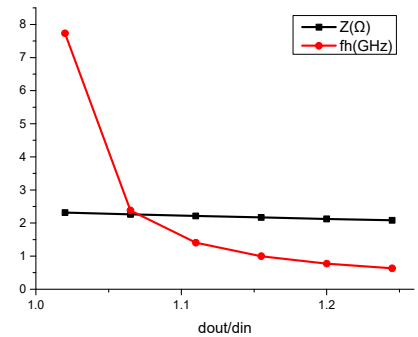

(a)

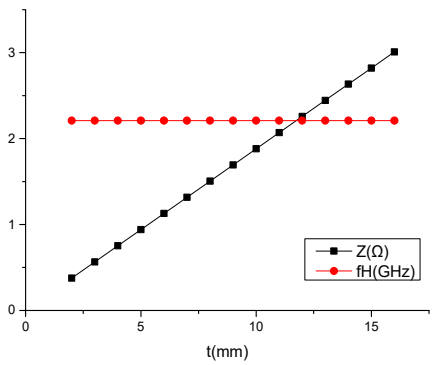

(b)

Figure 2: Analysis of different parameters of ceramic ring on its performance. (a) When t fixed, the influence of dout/din on f_H and characteristic impedance Z; (b) When din and dout fixed, the influence of t on f_H and Z.

Combining the din, dout and t on f_H and Z, the final ceramic ring size parameters are: din=200 mm, dout=225 mm, t=12 mm, at this time, corresponding to f_H =1.2375 GHz, C_{gap} =58.494 pF, Z=2.1986 Ω

Magnetic Ring Design

The design of magnetic materials mainly includes material selection, size calculation, and reasonable combination design of different material rings.

According to the investigation, 1K101 and 1K502A are selected. The size of the magnetic ring is 220*280*30 mm. Meanwhile, Since the permeability of magnetic materials changes with frequency, choosing a suitable combination of magnetic materials can greatly improve the working bandwidth of WCM. Considering the ceramic ring, signal pick-up resistance, magnetic ring and other factors,

First, a total of 4 magnetic rings are used, and the system impedance vs. frequency curve is analyzed under different combinations of magnetic rings, as shown in Fig. 3. It can be seen that when all four magnetic rings use nanocrystalline magnetic materials, WCM low-frequency response is particularly excellent; when all four magnetic rings use amorphous magnetic materials, WCM high-frequency response is particularly excellent; while combination two nanocrystalline and two amorphous magnetic materials, the bandwidth of the WCM is significantly improved. Obviously, the combination of two materials is better.

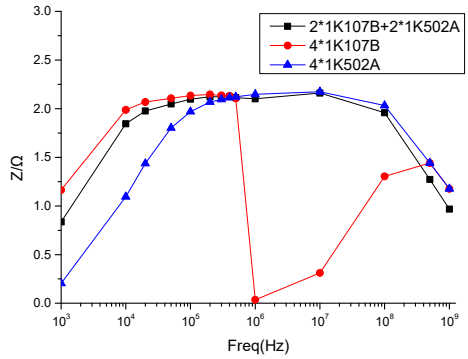

Figure 3: The impedance vs. frequency under different combinations of four magnetic rings.

In order to further broaden the WCM bandwidth, it is necessary to increase the inductance, which can only be achieved by increasing the volume of the magnetic ring or increasing the number of magnetic rings. Here, we choose to increase the number of magnetic rings to six and eight combinations. The WCM system impedance vs. frequency curve is shown in Fig. 4.

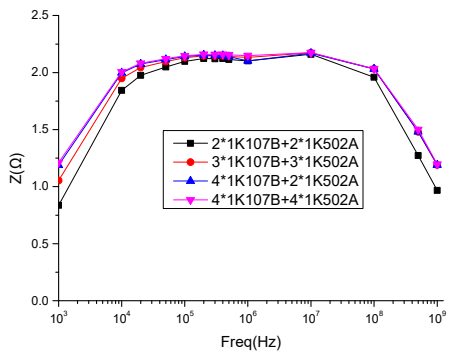

Figure 4: The impedance vs. frequency under combinations of four/six/eight magnetic rings.

It can be seen that the more the number of magnetic rings, the broaden the frequency band, but the total number is no longer improved significantly after the total number is increased from 6 to 8. And the system bandwidth of the combination of 4 nanocrystals and 2 amorphous magnetic materials is best. Therefore, finally choose 4*1K107B and

ISBN: 978-3-95450-230-1 ISSN: 2673-5350 doi:10.18429/JACoW-IBIC2021-WEPP23

2*1K502A magnetic ring combination, the theoretical 3dB working bandwidth of this WCM is 2 kHz~400 MHz.

Figure 5 shows the actual processed magnetic ring and the magnetic permeability test results of the magnetic ring.

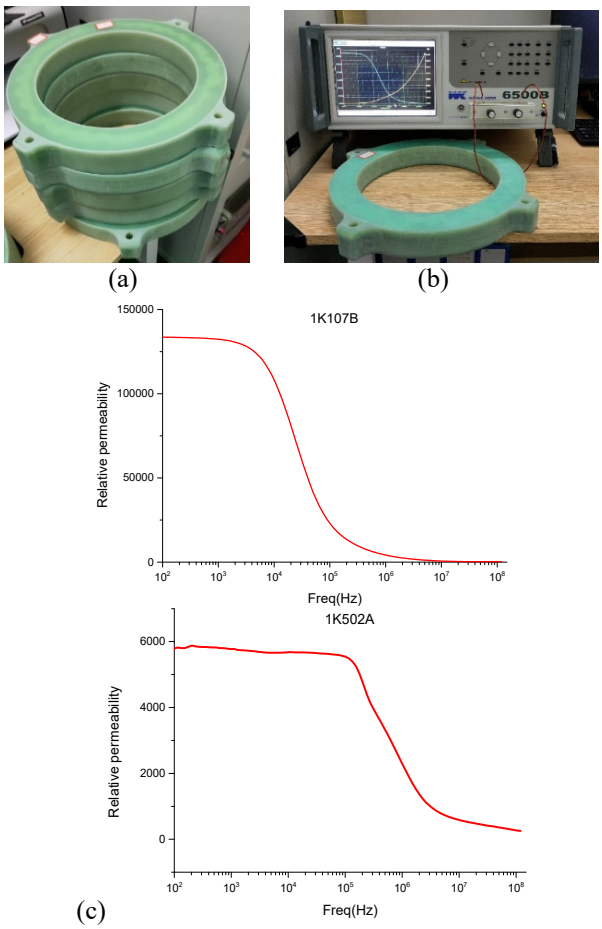

Figure 5: The actual magnetic ring processing and the magnetic permeability test results of the magnetic ring. (a) Magnetic ring finished product; (b) L-f performance test scenario; (c) The magnetic permeability of the two cores and the magnetic ring change curve with frequency.

Signal Pick-up Resistor Design

This part of the design directly affects the accuracy of the final extracted signal. Here, we choose a flexible circuit board to design a flexible resistance band for signal pickup.

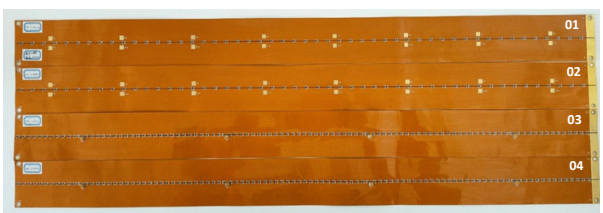

Figure 6: Physical picture of flexible resistance band.

The flexible resistance board material used Panasonic R-F777, and its equivalent resistance is 2.2 Ω. Two versions of the resistance board are designed, as shown in Fig. 6. 50 110 Ω resistors are used in parallel for circuit boards 01 and 02; the signal is led out by pads. 100 220 Ω resistors are used in parallel for circuit boards 03 and 04, the signal is led out by a patch-type SSMP connector, using a patch-type SSMP connector can effectively reduce the signal reflection at the connection compared with direct pad welding. The upper and lower copper-clad parts of the circuit board are connected by a number of metallized vias to ensure good electrical conduction between the resistance band and the vacuum pipeline.

Table 1: Measured Value of Equivalent Resistance Value of Flexible Resistance Band

Number	Test resistance(Ω)	Inherent error(Ω)	Actual resistance(Ω)
01	2.35	0.151	2.199
02	2.353	0.151	2.202
03	2.35	0.151	2.199
04	2.353	0.151	2.202

The theoretical design value of the equivalent resistance of the flexible resistance band is 2.2 Ω, the actual measured value is 2.2±0.002 Ω as shown in Table 1. The accuracy is controlled within one thousandth, which meets the design requirements.

WCM Mechanical Structure Design

Figure 7 shows the WCM mechanical structure, mainly considering from the aspects of mechanical processing and assembly, such as: strict control of the brazing process between the ceramic ring and the vacuum pipe, the fixing of the magnetic ring structure, the good conductive contact between the flexible resistance band and the stainless steel pipe, the reasonable installation position of each connector and the filling of the wave absorbing material, etc.

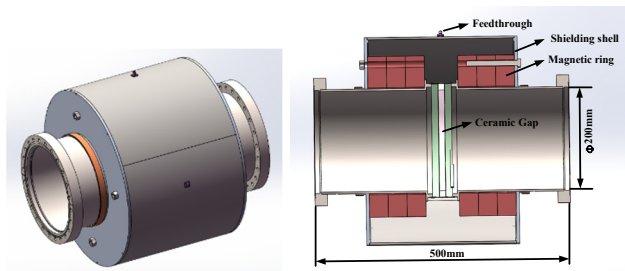

Figure 7: Three-dimensional drawing and cross-sectional view of the mechanical structure of WCM.

SIMULATION OF WCM

Calibration Platform Designer and Simulation

A calibration platform is needed to calibrating and testing for W[illegible]

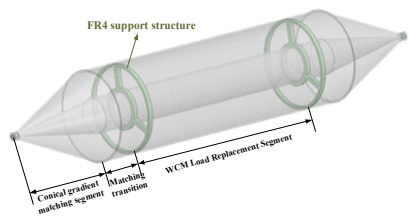

Figure 8: Simulation modal of calibration structure.

ISBN: 978-3-95450-230-1 ISSN: 2673-5350 doi:10.18429/JACoW-IBIC2021-WEPP23

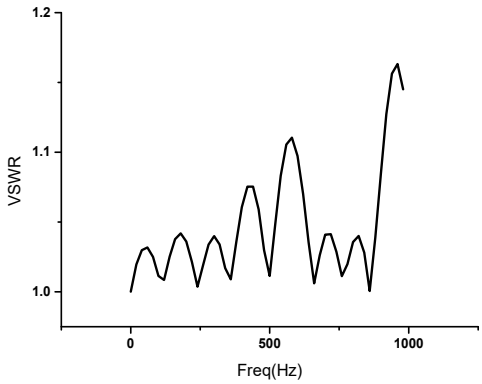

Figure 9: VSWR vs. frequency curve.

From the perspective of microwave transmission, a tapered gradual coaxial conversion structure is designed for offline calibration of the WCM, and the electromagnetic simulation software ANSYS HFSS software is used for design simulation calculations. The model structure is shown in Figs. 8 and 9 shows the VSWR vs. frequency curve of this coaxial in 0~1 GHz. The result shows that in the range of 0~400 MHz, VSWR≤1.05, the matching is excellent, which can be used for the calibration of WCM of this design.

WCM simulation analysis

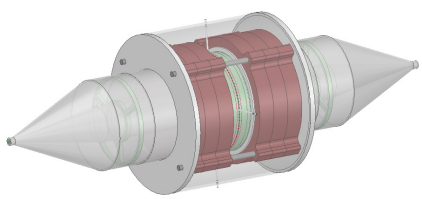

Figure 10: simulation model of WCM.

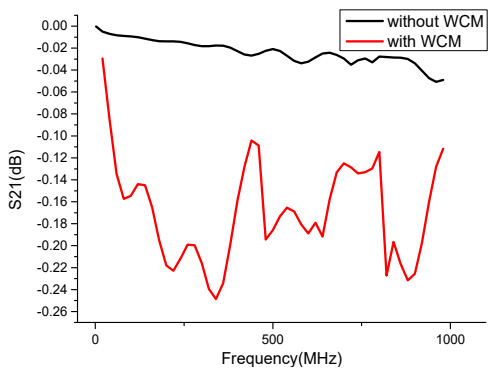

Figure 11: Frequency response curve.

The simulation model of WCM is shown in Fig. 10, its working bandwidth is analyzed. The result is shown in Fig. 11, the coaxial conversion structure (shown in Fig. 8), the transmission coefficient S21≥-0.05dB in the frequency range of 0~1 GHz. After loading the WCM structure (shown in Fig. 10), S21 drops slightly in the frequency range of 10 kHz to 1 GHz, but does not exceed 0.25 dB, which proves that the high energy transmission efficiency is in line with expectations.

DISCUSSION

There is still room for optimization in this solution [2]. For example, the flexible circuit board designed to bridge the signal pickup resistance can be integrated the function of microstrip power combiner, which can improve the reliability of the structure; The test verifies the current absorbing performance of the absorbing material in the range of 2 k~400 MHz. If it does not have a significant absorbing effect, we need to consider reducing the size of the cavity without adding absorbing materials or using a ferrite absorbing array solution [3].

CONCLUSION

This article comprehensively introduces the detailed design process of WCM for HIAF [4]. According to current theoretical calculations and simulation results, the working bandwidth of this WCM is 2 kHz~400 MHz. However, according to other WCM designs and test results investigated [1, 5, 6], compared with the design results, the measured working bandwidth will be better than the design bandwidth. At present, the WCM has completed the procurement and processing of various components, but due to time constraints, offline and online testing have not yet been carried out. It is expected to be installed at the Heavy Ion Research Facility in Lanzhou-Cooling Storage Ring (HIRFL-CSR) for online testing in August.

ACKNOWLEDGEMENT

Special thanks to Jilei Sun from Institute of High Energy Physics for his guidance and help in this design.

REFERENCES

[1] Sun Jilei *et al.*, “Design of the wall current monitor system at CSNS rapid cycling synchrotron[J]”, *High Power Laser and Particle Beams*, vol. 30, p. 125103, 2018. doi:10.11884/HPLPB201830.180224

[2] A. D’Elia, R. Fandos, and L. Søby, “High bandwidth Wall Current Monitor for CTF3”, in *Proc. 7th. European Particle Accelerator Conference. (EPAC’08)*, Genoa, Italy, June. 2008, pp. 1092-1094. doi:10.18429/JACoW-EPAC08-TUPC021

[3] B. Fellenz and J. Crisp, “An improved resistive wall monitor”, *American Institute of Physics*, vol. 451, pp. 446-453, 1998. doi:10.1063/1.57030

[4] Yang J C *et al.*, “High Intensity heavy ion Accelerator Facility (HIAF) in China”, *Nuclear Instruments and Methods in Physics Research Section B Beam Interactions with Materials and Atoms*, vol. 317, pp. 263-265, 2013. doi:10.1016/j.nimb.2013.08.046

[5] J.M. Belleman and W. Andreazza, “A New Wall Current Monitor for the CERN Proton Synchrotron”, in *Proc.5th. International Beam Instrumentation Conference. (IBIC’16)*, Barcelona, Spain, Sept. 2016, pp. 143-146. doi:10.18429/JACoW-IBIC2016-MOPG41

[6] P.Odier, “A New wide band Wall Current Monitor”, in *Proc. 6th. Beam Diagnostics and Instrumentation for Particle Accelerators. (DIPAC’03)*, Mainz, Germany, May. 2003, pp. 216-218. doi:10.18429/JACoW-DIPAC 2003-PT20